ACS APPLIED MATERIALS & INTERFACES

Research Article

www.acsami.org

Increasing Resistivity of Electrically Conductive Ceramics by Insulating Grain Boundary Phase

Takafumi Kusunose*,[†] and Tohru Sekino[‡]

[†]Department of Advanced Materials Science, Faculty of Engineering, Kagawa University, Hayashi-cho 2217-20, Takamatsu 761-0396, Japan

[‡]Institute of Multidisciplinary Research for Advanced Materials Tohoku University (IMRAM), Tohoku University, Katahira 2-1-1, Aoba-ku, Sendai 980-8577 Japan

Supporting Information

ABSTRACT: Increasing resistivity of electrically conductive nonoxide ceramics was investigated by insulating conductive pathways through conductive grains in a sintered body by addition of an insulating grain boundary phase, which was produced by the reaction of sintering additives in liquid phase sintering. When SiC was hot pressed with an additive of 10 vol % of Al_2O_3 and Y_2O_3, the resistivity decreased as sintering temperature increased owing to contact between SiC grains during densification. However, by hot pressing at 1750°C, a high resistivity of greater than 1×10^{11} Ω cm was achieved because of the penetration of an insulating grain boundary phase between the SiC grains. It is possible to fabricate high-resistivity SiC ceramics without losing their excellent mechanical properties by introduction of an insulating grain boundary phase, the volume of which is approximately 1/7 that of the insulating phase incorporated in conventional ceramic composites.

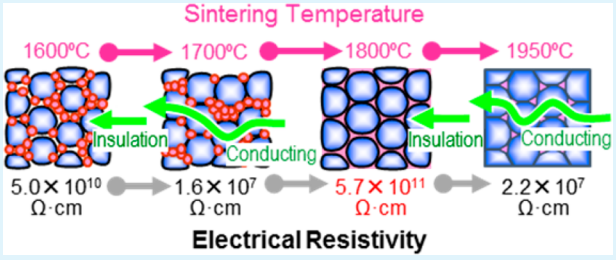

KEYWORDS: *silicon carbide, grain boundary phase, epoxy, hybrid material, thermal conductivity, insulation*

1. INTRODUCTION

Control of the electrical conductivity of structural ceramics has been studied for industrial applications. To impart electrical conductivity to insulating ceramics, dispersions of conducting second phase particles have been considered.[1−10] In such composites, conducting particle contents above 12−30 vol % are necessary to produce conducting ceramics. However, it has not been reported whether the resistivity of conductive ceramics can be increased by dispersion of insulating ceramic particles. From consideration of previous reports[1−10] regarding the promotion of conductivity in insulating ceramics, it is speculated that insulating second phase particle contents above 70 vol % would be necessary to increase the resistivity of conductive ceramics in the manner illustrated in Figure 1a. However, the addition of large amounts of a second phase is undesirable because this can potentially compromise the excellent mechanical properties of the matrix ceramics. Therefore, increasing the electrical resistivity of conductive ceramics by addition of smaller amounts of a second phase becomes important. Our group has reported that electrically conductive AlN can be fabricated by forming a conductive rare earth oxycarbide as a grain boundary phase.[11] The grain boundary phase three dimensionally propagates in the sintered body. By employing a continuous grain boundary phase as a conducting pathway, a grain boundary phase content below 3 vol % was sufficient to impart electrical conductivity to the insulating ceramic. In this conductive ceramic, the grain boundary phase concentrated at grain boundary pockets such as three points or multiple points and continuously propagated in the sintered body. It is a well-known property of liquid phase sintering that grain boundary phases aggregate at grain boundary pockets as sintering progresses. However, grain boundary phases also remain at facial boundaries just after densification.[12−14] If the insulating grain boundary phases can be precipitated not only at grain boundary pockets but also at the facial boundaries, as that illustrated in Figure 1b, it is expected that it would be possible to render conductive ceramics highly resistive without losing the intrinsic properties of the matrix ceramics.

Nonoxide ceramics, such as nitrides, carbides, and borides, have many advantageous mechanical properties at both room temperature and high temperatures due to strong covalent bonding. Additionally, most nonoxide ceramics except for AlN and Si_3N_4 are electrically conductive materials, exhibiting metallic conductivity or semiconductivity. In the category of nonoxide ceramics, SiC is a promising candidate for components in advanced gas turbines, piston engines, and heat exchangers because it possesses high strength and excellent creep resistance at elevated temperatures.[15,16] Recently, SiC ceramics have received considerable attention as a useful material for semiconductor manufacturing equipment in response to advancements in the development of SiC wide

Received: November 22, 2013
Accepted: January 28, 2014
Published: January 28, 2014

   dx.doi.org/10.1021/am4052766 | ACS Appl. Mater. Interfaces 2014, 6, 2759−2763

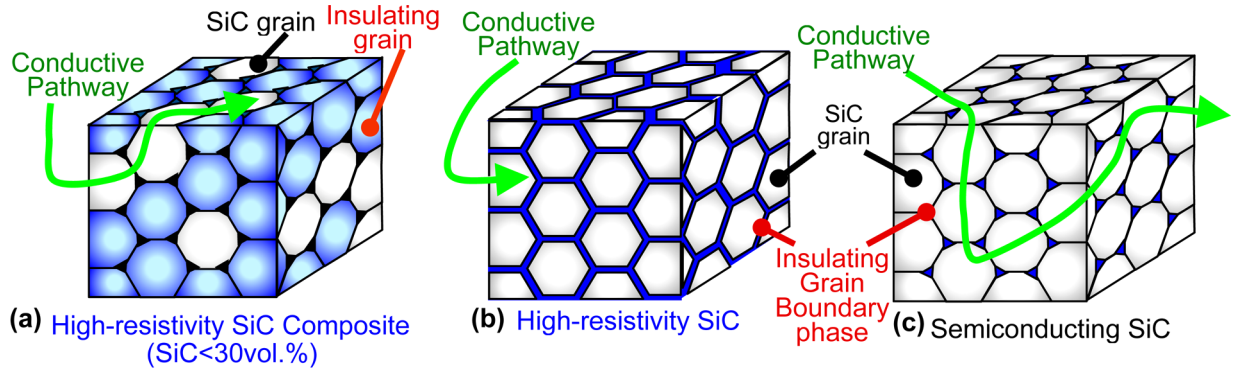

Figure 1. Models of conferring high resistivity to conductive ceramics. (a) A high-resistivity SiC composite created by dispersion of insulating second phase particles. The conductive pathways through SiC grains are disconnected by the insulating grains. (b) High-resistivity SiC. Semiconducting SiC grains are insulated by an insulating grain boundary phase. (c) Conventional liquid-sintered SiC ceramics exhibiting semiconductivity.

gap semiconductors, which offer electric devices operating with reduced power consumption.[17] Additionally, the electronic parts in semiconductor manufacturing equipment also require various electrical resistivities, e.g., electrostatic chucks require a resistivity of 1×10^{14} from 1×10^{8} Ω cm to provide sufficient adsorption force,[18] and vacuum chucks need a resistivity of approximately 1×10^{6} Ω cm to inhibit accumulation and discharge of static electricity. However, because the resistivity of conventional SiC ceramics is 1×10^{3} to 1×10^{5} Ω cm, increasing the resistivity of SiC ceramics while retaining the material's excellent mechanical properties is highly desirable for these applications.

For sintering strongly covalently bonded SiC, a combination of Al_2O_3 and Y_2O_3 (Al_2O_3–Y_2O_3) or B and C (B–C) of several volume percentage is added as a sintering aid. In the case of the B–C additive, the densification of SiC is achieved by solid state sintering.[19,20] On the other hand, in the case of the Al_2O_3–Y_2O_3 additive, densification proceeds through liquid phase sintering. Al_2O_3 and Y_2O_3 produce liquid phases during sintering by reacting with silicon oxide found on SiC,[21−24] and, after sintering, the liquid phase transforms into an insulating grain boundary phase such as yttrium silicate and/or yttrium aluminate and a small amount of amorphous phase. It is thought possible that the resistivity of SiC can be increased by insulating the contacts between the conductive SiC grains using an insulating grain boundary phase, as shown in Figure 1b.

In this study, liquid phase sintering of SiC was investigated to develop a method for increasing resistivity of electrically conductive ceramics using insulating grain boundary phases. To increase the resistivity of SiC without losing its excellent mechanical properties, sintering conditions and the amount of additives were optimized to precipitate the insulating phase at the facial boundaries as well as at grain boundary pockets. It has been reported that the resistivity of SiC ceramics was increased by sintering with BeO because of minimization of carrier concentration in SiC grains.[24] This method is applicable to only SiC and may not be applicable to other conductive nonoxides. However, the proposed method for increasing the resistivity of conductive ceramics by incorporating a grain boundary phase can be potentially applied to any nonoxide ceramic that can be densified by liquid phase sintering.

2. EXPERIMENTAL PROCEDURES

A combination of Al_2O_3 and Y_2O_3 was selected as a sintering additive because these compounds are well-known to produce insulating grain boundary phases, additionally to improve the mechanical properties of sintered SiC ceramics, compared with a combination of B and C additives. The content of Al_2O_3–Y_2O_3 was adjusted to 5, 7.5, 10, and 15 vol %, where the molar ratio of Al_2O_3 and Y_2O_3 was fixed at Al_2O_3/Y_2O_3 = 3/5. Commercially available SiC powder (UF-25, H. C. Starck , Karlsruhe, Germany), Al_2O_3 powder (TM-DAR grade, Taimei Chemical Co., Ltd., Tokyo, Japan), and Y_2O_3 powder (OR, Shin-Etsu Chemical Co., Ltd., Tokyo, Japan) were mixed by conventional wet ball milling with Si_3N_4 balls and ethanol for 24 h to obtain a homogeneous mixture. After drying, the powders were dry ball milled for 6 h to eliminate hard agglomerations. The powder mixtures were placed in a graphite die coated with a BN slurry to avoid reaction between the powders and the die. Hot pressing was performed from 1600 to 1950°C for 1 h in an argon atmosphere under uniaxially applied pressure of 30 MPa. The obtained hot-pressed samples, which were 44 mm in diameter and 5 mm in thickness, were cut with a diamond saw, ground with a diamond whetstone, and polished with a 0.5 μm diamond slurry for use in various evaluations.

The crystalline phases of the sintered SiC and additives were determined by X-ray diffractometry (XRD) using Cu Ka radiation (XRD-6100, Shimadzu Co., Ltd, Kyoto, Japan). The relative density was measured by the Archimedes method via immersion in toluene. The theoretical density was calculated using the specific gravity of 3.21 for SiC, 3.99 for Al_2O_3, and 5.03 for Y_2O_3. The microstructure was observed by scanning electron microscopy (SEM, Model S-5000, Hitachi, Tokyo, Japan) on polished and CH_4 gas plasma-etched surfaces to reveal the morphologies and locations of SiC grains and grain boundary phases. The DC electrical resistivity of the samples was measured by 2-probe method using a Keithley electrometer (model 6517, Keithley Instruments Inc., Ohio, USA) computer controlled by the 6524 software package at room temperature. The electrodes were formed on the upper and lower side of the disk by painting on silver paste. To exclude a surface current effect, a guard ring was also formed around the lower side electrode. The electrical resistivity distributions on the sample surfaces were visualized using a surface potential image obtained by electrostatic force microscopy (EFM) in conjunction with scanning probe microscopy (SPM, Nanoscope IIIa, Veeco Instruments, New York, USA). The sample size for EFM was 2 mm × 2 mm × 1.5 mm, and its surface was polished using a diamond slurry to a surface roughness of under 0.5 nm (= Ra). For EFM analysis, a probe composed of silicon scanned a 3 μm × 3 μm region of the sample surface by a noncontact mode, frequency modulation method of electrical force microscope testing in which a DC bias voltage of 8 V was applied at the probe. Young's modulus of 2 mm × 4 mm × 37 mm specimens was determined by a resonance vibration method with first-mode resonance. Fracture strength was evaluated by three-point bending test. At least 4 specimens were tested for each sample to determine an average of fracture strength. The specimen thickness, span length, and crosshead speed were 3 mm, 30 mm, and 0.5 mm/min, respectively.

3. RESULTS AND DISCUSSIONS

3.1. Fabrication of SiC Ceramics with High Resistivity.

Figure 2 shows the relative densities of sintered SiC and

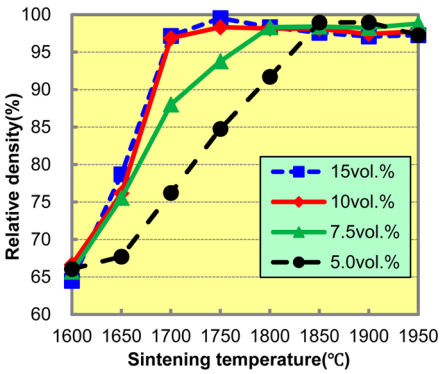

Figure 2. Relative density as a function of sintering temperature for SiC hot pressed with Al_2O_3–Y_2O_3 additives of 5 (black circle), 7.5 (green triangle), 10 (red diamond), and 15 vol % (blue square).

additive mixtures as a function of sintering temperature. High densifications of the SiC powder mixtures containing 5, 7.5, 10, and 15 vol % additives were observed at 1850, 1800, and 1750 °C. The densification behavior was greatly affected by the additive content, wherein increases in the additive content enhanced densification. It is well-known that oxide additives form liquid phases by reacting with oxide components of the nonoxide matrix ceramic powder during the initial step of densification in liquid phase sintering.[25] It is considered that the observed densification of the SiC mixtures containing additives of higher volume percent was promoted because of diffusion and deformation of the reactants such as yttrium silicates and yttrium aluminates, which are derived from the additives and have lower melting points than SiC. Figure 3 shows the XRD patterns of the sintered SiC samples including 10 vol % an additive, which have been hot pressed at temperatures from 1600 to 1900 °C for 1 h. The figure illustrates the transformation of crystalline phase of grain boundary phases in the SiC sintered body depending on the sintering temperature. Yttrium silicate (Y_2SiO_5) and yttrium aluminate

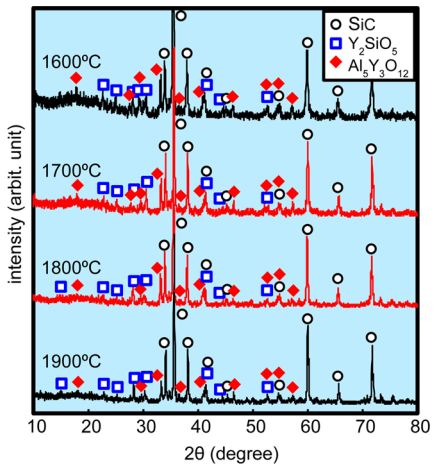

Figure 3. XRD profiles of SiC containing 10 vol % of an Al_2O_3–Y_2O_3 additive hot pressed at various sintering temperatures between 1600 and 1900 °C for 1 h in argon, showing the transformation to a crystalline grain boundary phase.

($Al_5Y_3O_{12}$), mainly produced by reactions involving additives, were identified as grain boundary phases, even in the sample sintered at 1600 °C. All the observed crystalline grain boundary phases were insulators with resistivities greater than 1×10^{13} Ω cm.

3.2. Electrical Resistivity and Microstructure of SiC.

Figure 4 plots the electrical resistivity of sintered SiC with varying additive contents and sintering temperatures. The electrical resistivity of the hot-pressed SiC ceramics increased with additive content. The SiC ceramics hot pressed from 1600 to 1700 °C tended to decrease in resistivity with a rise in sintering temperature because of the formation of conducting pathways by contacts between SiC grains during densification. However, sudden increases in resistivity were observed in the sample sintered at 1750 °C, where it is considered that the conducting pathways through SiC grains were disconnected by incorporation of insulating grain boundary phases between SiC grains. As represented in Figure 5a–c, the localization of the additive oxides and small pores was observed in the microstructure of SiC with 10 vol % additive sintered at 1700 °C, where it appears that the liquid phase does not sufficiently penetrate between SiC grains. However, by sintering between 1750 and 1850 °C, the localization of the liquid phase and small pores disappeared, and the grain boundary phase is observed to penetrate around the SiC grains. At higher sintering temperatures, the grain boundary phase migrated to triple or multiple points from the circumferences of SiC grains with grain growth, as shown in Figure 5d, and resistivity decreased again because of contact between SiC grains.

The electrical resistivity on the sample surface, indicative of different materials, can be observed by the surface potential image obtained by EFM. Images a and b in Figure 6 indicate SPM and surface potential images, respectively, of high-resistivity SiC, which was fabricated by hot pressing with 10 vol % additive at 1850 °C. Because this sample has a high bulk resistivity of 5.7×10^{11} Ω cm, measurement by noncontact mode was adopted to obtain a surface potential image. From the surface potential image, it is possible to determine the extent to which the grain boundary phase insulates the conducting pathways of connected SiC grains. The resistivity of the surface can be estimated from the surface potential image by the brightness levels, wherein dark and bright regions correspond to materials having high and low electrical resistivities, respectively.[26] Comparison of the surface potential image with the SPM image indicates that the resistivity of the surrounding grain boundary phase was higher than that of the SiC grains. The enhancement of the resistivity of the sample can therefore be attributed to a breakdown of the conducting pathways constituted from connected SiC grains by incorporation of the insulating grain boundary phase between SiC grains. The data suggest that the liquid phase produced by the reaction of the sintering additives and silicon oxide homogeneously penetrates around SiC grains by capillary force at approximately 1750 °C, and, after sintering, the liquid phase remains as an insulating grain boundary phase, such as Y_2SiO_5, $Al_5Y_3O_{12}$, and an amorphous phase, around the SiC grains.

Mechanical properties of high-resistivity SiC. Figure 7 shows the variation of Young's modulus and fracture strength with sintering temperature for the SiC hot pressed with the Al_2O_3–Y_2O_3 additive. Young's modulus of both high-resistivity SiC and low-resistivity and SiC increased with density. Since Young's modulus of SiC is higher than that of the grain boundary phase,

dx.doi.org/10.1021/am4052766 | ACS Appl. Mater. Interfaces 2014, 6, 2759–2763

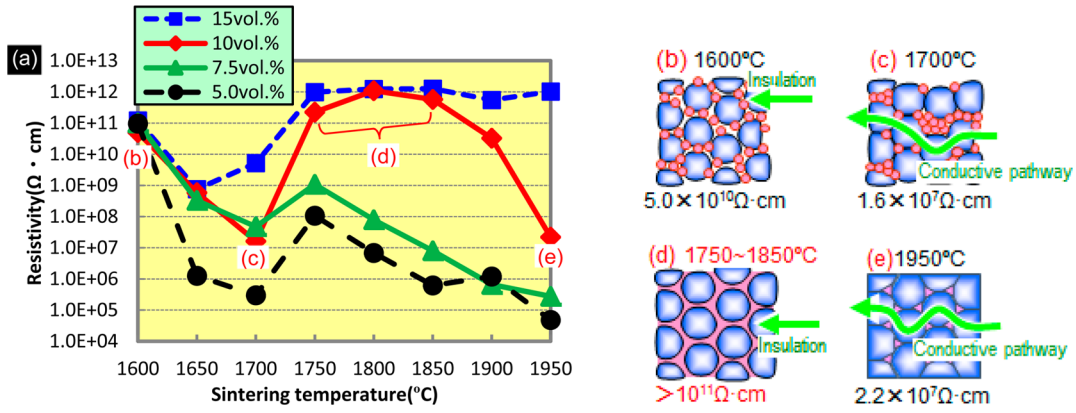

Figure 4. (a) Relationship between electrical conductivity and sintering temperature for SiC samples sintered with different additive contents. Predicted microstructure and conductive pathway of SiC containing 10 vol % of an Al_2O_3–Y_2O_3 additive hot pressed at (b) 1600, (c) 1700, (d) 1750–1850, and (e) 1950 °C.

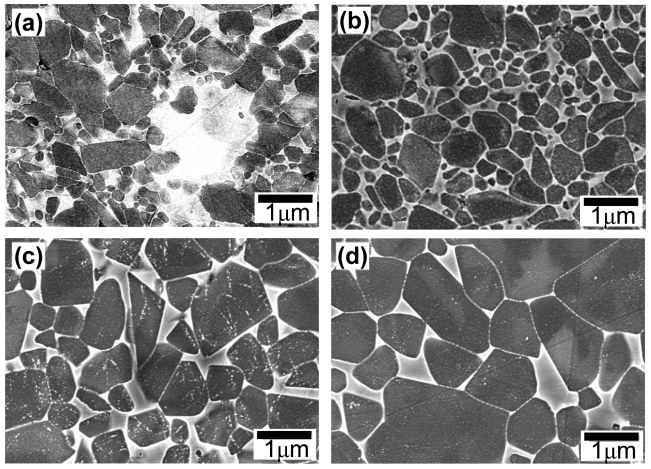

Figure 5. SEM micrographs of polished and etched surfaces of SiC containing 10 vol % Al_2O_3–Y_2O_3 additive hot pressed at (a) 1700, (b) 1750, (c) 1850, and (d) 1950 °C. Dark grains and bright phases between dark grains correspond to SiC grains and grain boundary phases, respectively.

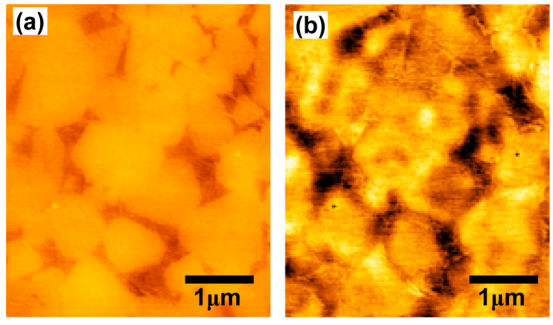

Figure 6. (a) SPM image and (b) the corresponding surface potential image of sintered SiC containing 10 vol % Al_2O_3–Y_2O_3 additive hot pressed at 1850 °C.

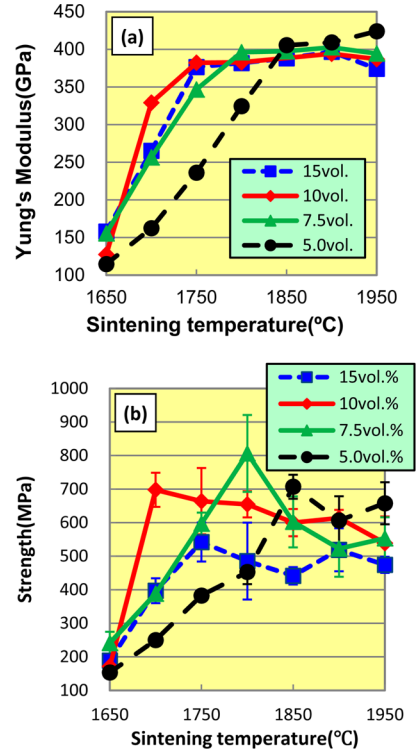

Figure 7. Effect of the sintering temperature on (a) Young's modulus and (b) fracture strength of SiC hot pressed with 5 (black circle), 7.5 (green triangle), 10 (red diamon), and 15 vol % (blue square) Al_2O_3–Y_2O_3 additives.

the SiC containing smaller amounts of the additive provided a higher Young's modulus. However, it was discovered that even high-resistivity SiC containing 10 or 15 vol % additive had a high Young's modulus of more than 380 GPa, which is approximately equal to that of Al_2O_3[27] and is higher than that of Si_3N_4.[28] The fracture strength of SiC has a correlation with the relative density and Young's modulus. In general, the densified SiC samples with high Young's modulus and small grain size indicate high strength. By sintering at high temperatures, the decrease in fracture strength is attributed to the grain growth of SiC. Although SiC containing 15 vol % additive did not demonstrate high strength because of higher content of the grain boundary phase, the strength is higher than about 350 MPa of conventional SiC sintered with B–C additives.[29,30] SiC with an additive of 10 vol % and a resistivity of more than 1×10^{11} Ω cm demonstrated high strength between 600 and 670 MPa.

dx.doi.org/10.1021/am4052766 | ACS Appl. Mater. Interfaces 2014, 6, 2759–2763

4. CONCLUSIONS

The resistivity of SiC hot pressed with Al_2O_3–Y_2O_3 additives from 1600 to 1700 °C decreased as sintering temperature increased owing to contacts between the SiC grains by shrinkage during densification. However, the resistivity suddenly increased when hot pressed at 1750°C, where it is considered that the conducting pathways through SiC grains were disconnected by penetration of an insulating grain boundary phase between the grains. The additive of only 10 vol % increased the resistivity of the SiC sintered body from 1×10^5 to 1×10^{11} Ω cm by electrically insulating the regions between SiC grains by means of a grain boundary phase without losing the excellent mechanical properties of the matrix ceramic. An increase in the electrical resistivity of semiconducting materials is also somewhat possible by reducing charge carrier concentrations by adding dopants. This method is limited to semiconductors and, in application of the method, it is necessary to investigate effective dopants for every semiconductor. On the other hand, increasing the electrical resistivity by incorporation of a grain boundary phase is potentially applicable to not only semiconducting ceramics but also metallic conductive ceramics, which are densified through liquid phase sintering.

■ ASSOCIATED CONTENT

Supporting Information

Additional figure (PDF). This material is available free of charge via the Internet at http://pubs.acs.org.

■ AUTHOR INFORMATION

Corresponding Author

*E-mail: kusuno15@eng.kagawa-u.ac.jp. Tel. & Fax: +81-87-864-2401.

Notes

The authors declare no competing financial interest.

■ ACKNOWLEDGMENTS

The authors thank Mr. Kazuki Sakawa (Department of Advanced Materials Science, Kagawa University) for help with sample preparation, and UBE Scientific Analysis Laboratory Inc. for EFM analysis. This work supported by the Japan Society for the Promotion of Science (JSPS) under the Grant-in-Aid for Scientific Research (B).

■ REFERENCES

(1) Vanmeensel, K.; Laptev, A.; Van der Biest, O.; Vleugels, J. *Acta Mater.* **2007**, *55*, 1801–1811.
(2) Jin, X.; Gao, L. *J. Am. Ceram. Soc.* **2006**, *89*, 1129–1132.
(3) Zivkovic, L.; Nikolic, Z.; Boskovic, S.; Miljkovic, M. *J. Alloys Compd.* **2004**, *373*, 231–236.
(4) Gao, L.; Li, J.; Kusunose, T.; Niihara, K. *J. Eur. Ceram. Soc.* **2004**, *24*, 381–386.
(5) Duan, R.-G.; Garay, J. E.; Kuntz, J. D.; Mukherjee, A. K. *J. Am. Ceram. Soc.* **2004**, *88*, 66–70.
(6) Kawano, S.; Takahashi, J.; Shimada, S. *J. Am. Ceram. Soc.* **2003**, *86*, 701–705.
(7) Luo, Y. M.; Li, S. Q.; Chen, J.; Wang, R. G.; Li, J. Q.; Pan, W. *J. Am. Ceram. Soc.* **2002**, *85*, 3099–3101.
(8) Zhou, M.; Zhong, J.; Zhao, J.; Rodorigo, D.; Cheng, Y. B. *Mater. Res. Bull.* **2013**, *48*, 1927–1933.
(9) Krupa, M. S.; Kumar, N. D.; Kumar, R. S.; Chakravarthy, P.; Venkateswarlu, K. *Ceram. Int.* **2013**, *39*, 9567–9574.
(10) Kim, K. J.; Kim, K. M.; Kim, Y. W. *J. Eur. Ceram. Soc.* **2014**, *34*, 1149–1154.
(11) Kusunose, T.; Sekino, T.; Niihara, K. *Acta mater.* **2007**, *55*, 6170–6175.
(12) Pezzotti, G.; Nakahira, A.; Tajika, M. *J. Eur. Ceram. Soc.* **2000**, *20*, 1319–1325.
(13) Foster, D.; Thompson, D. P. *J. Eur. Ceram. Soc.* **1999**, *19*, 2823–2831.
(14) Falk, L. K. L. *J. Eur. Ceram. Soc.* **1997**, *17*, 983–994.
(15) Chen, D.; Sixta, M. E.; Zhang, X. F.; De Jonghe, L. C.; Ritchie, R. O. *Acta Mater.* **2000**, *48*, 4599–4608.
(16) Ishikawa, T.; Kohtoku, Y.; Kumagawa, K.; Yamamura, T.; Nagasawa, T. *Nature* **1998**, *391*, 773–775.
(17) Casady, J. B.; Johnson, R. W. *Solid-State Electron.* **1996**, *39*, 1409–1422.
(18) Watanabe, T.; Kitabayashi, T. *J. Ceram. Soc. Jpn.* **1992**, *100*, 1–6.
(19) Datta, M. S.; Bandyopadhyay, A. K.; Chaudhuri, B. *Bull. Mater. Sci.* **2002**, *25*, 181–189.
(20) Vaßen, R.; Kaiser, A.; Förster, J.; Buchkremer, H. P.; Stöver, D. *J. Mater. Sci.* **1996**, *31*, 3623–3637.
(21) Sciti, D.; Bellosi, A. *J. Mater. Sci.* **2000**, *35*, 3849–3855.
(22) She, J. H.; Ueno, K. *Mater. Res. Bull.* **1999**, *34*, 1629–1636.
(23) Padture, N. P. *J. Am. Ceram. Soc.* **1994**, *77*, 519–523.
(24) Ogihara, S.; Maeda, K.; Takeda, Y.; Nakamura, K. *J. Am. Ceram. Soc.* **1985**, *68*, c-16–c-18.
(25) Can, A.; Herrmann, M.; McLachlan, D. S.; Sigalas, I.; Adler, J. *J. Eur. Ceram. Soc.* **2006**, *26*, 1707–1713.
(26) Gheno, S. M.; Hasegawa, H. L.; Pimentel, V. L.; Filho, P. I. P. *J. Mater. Sci.* **2005**, *40*, 4641–4643.
(27) Kusunose, T.; Kim, Y. H.; Sekino, T.; Matsumoto, T.; Tanaka, N.; Nakayama, T.; Niihara, K. *J. Mater. Res.* **2005**, *20*, 183–190.
(28) Kusunose, T.; Sekino, T.; Choa, Y. H.; Niihara, K. *J. Am. Ceram. Soc.* **2002**, *85*, 2678–2688.
(29) Magnani, G.; Brentari, A.; Burresi, E.; Raiteri, G. *Ceram. Int.* **2014**, *40*, 1759–1763.
(30) Hannink, R. H. J.; Bando, Y.; Tanaka, H.; Inomata, Y. *J. Mater. Sci.* **1988**, *23*, 2093–2101.